Protein Components of the Backbone Structure of Postsynaptic Density of Type I Excitatory Synapses

Weiheng GUO[1], Qian LIU[1] and Tatsuo SUZUKI[1)2)]*

1) *Department of Neuroplasticity, Institute of Pathogenesis and Disease Prevention, Shinshu University Graduate School of Medicine*
2) *Department of Biological Sciences for Intractable Neurological Diseases, Institute for Biomedical Sciences, Interdisciplinary Cluster for Cutting Edge Research, Shinshu University*

Postsynaptic density (PSD) is a dynamic structure that functions as an essential device for synaptic transmission and plasticity, and is critical for normal synaptic and brain activities. Many neuropsychiatric diseases and symptoms appear to be caused by abnormalities in synapses, including PSD. Therefore, precise and detailed knowledge of PSD is valuable for understanding neuropsychiatric diseases and developing new therapies. In this paper, we searched for PSDs with lattice- or mesh-like structures by preparing PSD from rat forebrains using different detergents, brain ages, and methods for collecting the brains. We next searched for the protein components responsible for the mesh-like structure in PSD using sodium dodecyl sulfate polyacrylamide gel electrophoresis/silver staining coupled with mass spectrometry and quantitative analyses of western blotting. The results suggest that general cytoskeletal proteins, together with PSD scaffold and adaptor proteins, may play a role in the core structure of mature PSDs. In the immature PSD core, general cytoskeletal proteins, in particular actin and α-internexin, and synapse-associated protein 102 may be involved. However, Ca^{2+}/calmodulin-dependent protein kinase II is not a major constituent of the mesh-like PSD basic structure. *Shinshu Med J 65 : 211—224, 2017*

(Received for publication March 3, 2017 ; accepted in revised form April 10, 2017)

Key words : molecular architecture, postsynaptic density, type I synapse, postsynaptic density lattice, synaptic plasticity

Abbreviations : α-IN, α-internexin ; CaMKII, Ca^{2+}/calmodulin-dependent protein kinase II ; CaMKII α, α subunit of CaMKII ; CaMKII β, β subunit of CaMKII ; NF, neurofilament ; DOC, deoxycholate ; IAA, iodoacetamide ; LN, liquid nitrogen ; OG, n-Octyl-β-D-glucoside ; PSD, postsynaptic density ; SPM, synaptic plasma membrane ; TX-100, Triton X-100

I Introduction

The synapse is an essential element in neuronal networks and brain activity, and postsynaptic density (PSD) is a major structure in the postsynaptic side of the synapse. PSD is a special cytoskeleton localized immediately underneath the postsynaptic membrane and plays an important role in signal processing upon receiving neurotransmitters, which is related to the generation of synaptic plasticity. It is well known that abnormalities in synaptic and PSD proteins are related to neuropsychiatric disorders and mental retardation[1)-3)]. Therefore, detailed knowledge of PSD will provide a valuable clue to understand and develop new therapies for neuropsychiatric disorders. Indeed, PSD is a dynamic structure and the shape and size of both PSD and spines change when long-term potentiation (LTP) or long-

* Corresponding author : Tatsuo Suzuki
Department of Neuroplasticity, Institute of Pathogenesis and Disease Prevention, Shinshu University Graduate School of Medicine, 3-1-1 Asahi, Matsumoto Nagano 390-8621, Japan
E-mail : suzukit@shinshu-u.ac.jp

term depression (LTD) are induced[4]. The PSD, in particular the excitatory type I, has been extensively studied and is reported to consist of several hundreds to a thousand kinds of proteins. It is now believed that PSD comprises various scaffold and adaptor proteins-the scaffold/adaptor assembly model. In this model, PSD is constituted of the following three layers : (1) a surface layer containing receptors, channels, and cell adhesion molecules ; (2) a layer immediately underneath the postsynaptic membrane containing PSD-95 ; and (3) a layer consisting of ProSAP/Shank. The second and third layers are connected mainly by the guanylate kinase-associated protein (GKAP)/SAP-associated protein (SAPAP) adaptor protein. Among the scaffold and adaptor proteins, the Shank/ProSAP family is considered one of the master scaffold and adaptor proteins in PSD, and it nucleates the underlying structure of PSD[5]. The assembly of these scaffold and adaptor proteins is believed to form the lattice-like basement structure for the type I excitatory PSD (PSD lattice). However, there has been no direct evidence for this concept, and a detailed relationship between the scaffold/adaptor assembly model of the PSD architecture and the PSD lattice is not clear.

In this paper, we investigated major components of PSDs prepared from rat forebrains under various conditions, in which the mesh-like structure, possibly the PSD backbone structure, was observed in electron microscopy. This study is an initial survey to elucidate the relationship between the scaffold/adaptor assembly model and the PSD lattice, and to determine the protein components responsible for the backbone structure of PSD.

Ⅱ Materials and Methods

A Materials

Triton X-100 (TX-100), iodoacetamide (IAA), and ImmunoStar LD were purchased from WAKO Pure Chemical Industries Ltd. (Osaka, Japan), n-Octyl-β-D-glucoside (OG) from Dojindo Laboratories (Kumamoto, Japan), protease inhibitor cocktail (P8340) from Sigma-Aldrich (Saint Louis, MO), pepsin (S3002) from DAKO (Carpinteria, CA, USA) and Nano-W from Nanoprobes, Inc. (Yaphank, NY, USA). Antibodies used in this study are listed in **Table 1**. All other chemicals were of reagent grade.

B Preparation of synaptic plasma membranes (SPMs) and various kinds of PSDs

Animals were handled according to the Regulations for Animal Experimentation of Shinshu University. The animal protocol, together with animal handling, was approved by the Committee for Animal Experiments of Shinshu University (Approval Number 240066). Based on the national regulations and guidelines, all experimental procedures were reviewed by the Committee for Animal Experiments and finally approved by the president of Shinshu University.

SPMs were prepared from Wistar rats (males, 6 weeks old, specific pathogen-free ; Japan SLC, Inc., Hamamatsu, Japan), essentially as described previously[6]. Forebrains were collected on ice for 15 to 30 min after dissection and then saved at -80 ℃. In some cases, the forebrains (only 6-week-olds) were rapidly frozen with liquid nitrogen (LN) immediately following dissection (snap frozen) or treated at 37 ℃ for 5 min to prepare thin or thick PSDs, respectively. Preparations using forebrains without snap freezing or 37 ℃ treatment are defined as "regular preparation" in this paper. Buffers A and B[6] were supplemented with 2 mM IAA to prevent artificial oxidative cross-linking during the preparation of SPMs. Purified SPMs were stored unfrozen in buffers containing 50% glycerol at -30 ℃. Longer storage at -80 ℃ did not cause any deterioration of the samples for this experiment.

PSDs were prepared from stored SPMs by the method reported previously[7]. The flow chart in **Fig. 1** summarizes this method, which is suitable for the efficient preparation of various kinds of PSDs from small amounts of brains and SPMs. In brief, PSDs were isolated as pellets after treatment of SPMs (500 μg protein/1.75 mL) with TX-100 or OG in 20 mM Tris-HCl (pH 7.4) containing 150 mM NaCl and 1 mM EDTA (TNE buffer), followed by sucrose density gradient centrifugation[8)9)]. TX-100 and OG have been used for purification of PSD before. We

Table 1　List of antibodies used in this study

Antibody	species of antibody	dilution*	Product Code	Provider
anti-actin	Mouse	1/600	pan Ab-5	Thermo Scientific (Cheshire, UK, USA)
anti-α-IN	Rabbit	1/100,000	AB5354	Chemicon International (Billerica, MA)
anti-CaMKII	Mouse	1/2,000	611292	Transduction Laboratories (Lexington, KY, USA)
anti-chapsyn110	Rabbit	1/2,000	PA1-043	Thermo Scientific (Rockford, IL, USA)
anti-fodrin (non-erythroid α-spectrin)	Mouse	1/500	MAB1685	Chemicon International (Billerica, MA, USA)
anti-Homer	Goat	1/400	sc-8921	Santa Cruz Biotechnology Inc. (Santa Cruz, CA, USA)
anti-NF-H/Neurofilament 200	Rabbit	1/5,000	N4142	Sigma-Aldrich (Saint Louis, MO, USA)
anti-NF-M/Neurofilament 150	Rabbit	1/6,000	AB1981	Chemicon International (Billerica, MA, USA)
anti-NF-L/Neurofilament 70	Mouse	1/300	MAB1615	Chemicon International (Billerica, MA, USA)
anti-PSD-95	Mouse	1/1,000	610496	Transduction Laboratories (Lexington, KY, USA)
anti-SAP97	Mouse	1/1,000	VAM-PS005	StressGen Biotechnologies Corp (Victoria, BC, Canada)
anti-SAP102	Mouse	1/1,000	N19/2	UC Davis/NIH NeuroMab Facility (Davis, CA, USA)
anti-SAPAP/GKAP	Mouse	1/500	N127/31	UC Davis/NIH NeuroMab Facility (Davis, CA, USA)
anti-Shank1	Mouse	1/100	N22/21	UC Davis/NIH NeuroMab Facility (Davis, CA, USA)
anti-Shank2	Mouse	1/100	N23B/6	UC Davis/NIH NeuroMab Facility (Davis, CA, USA)
anti-tubulin	Rabbit	1/100,000		produced in a rabbit using pig tubulin as antigen

*Membranes were incubated with primary antibodies usually at 4℃ overnight. Dilutions are typical ones.

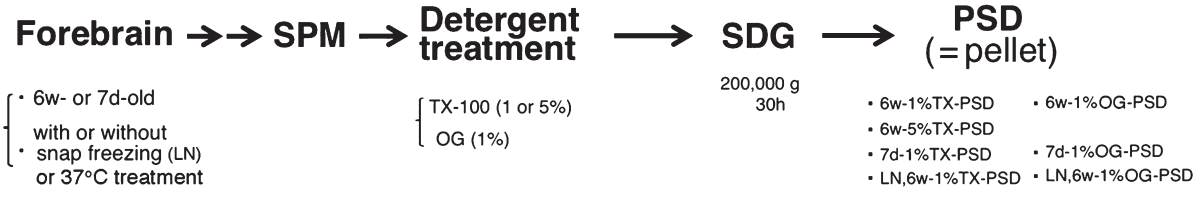

Fig. 1　Flow chart of the preparation of various types of PSDs.

Forebrains of 6-week-old or 7-day-old rats were used. Forebrains were dissected, placed on ice, and subsequently frozen or snap frozen with LN. The preparations using forebrains without snap freezing or 37℃ treatment are "regular preparation". SPM was treated with either TX-100 or OG. Under combinations of different conditions, various types of PSDs were prepared. Different types of PSDs used for identification of mesh-like structures in this study are listed. SDG refers to sucrose density gradient centrifugation. PSDs, postsynaptic densities ; LN, liquid nitrogen ; SPM, synaptic plasma membrane ; TX, Triton X ; OG, n-Octyl-β-D-glucoside.

prepared two-types of PSDs (TX-100-PSD and OG-PSD), since we thought that components essential for backbone structures of PSD may be commonly present in these different kinds of backbones. All PSD pellets were resuspended in 955 μl of TNE buffer. Detergent treatments were supplemented with protein inhibitor mixtures (P8340 ; Sigma-Aldrich) at 1/200 dilution along with IAA (2 mM).

C Electron microscopy

Electron microscopy was carried out as described previously[9]. Briefly, samples were fixed with 1% glutaraldehyde, postfixed with 1% osmiumtetroxide, dehydrated, and embedded in Epon. An ultrathin section was cut and stained with uranyl acetate and lead citrate. For the negative staining, 5 μl of the samples was spotted for a few to 15 min to glow-discharged formvar/carbon-coated copper grids at 0 ℃, and then excess liquids were blotted using a pipette. Grids were then negatively stained by placing them on 5 μl of Nano-W (Methylamine Tungstate) at room temperature twice according to the manufacturer's instructions. Specimens were examined under a JEOL JEM-1400EX (Tokyo, Japan) electron microscope at 80 kV. Contrast and sharpness (unsharp mask) of images were modified using Photoshop if a clearer visualization of the image was required.

D Analyses of protein and western blotting

For protein profiling, each PSD preparation was separated via sodium dodecyl sulfate polyacrylamide gel electrophoresis (SDS-PAGE) and the gels were stained with silver. Western blotting was carried out using a chemiluminescent substrate and visualized with a CCD video camera system (Atto Densitograph Lumino CCD AE-6930, ATTO Bioscience & Technology, Tokyo). Chemiluminescence of each band was measured by ATTO Lane analyzer 10H (Atto Bioscience & Biotechnology, Tokyo). Statistical analyses were performed using GraphPad Prism version 4.00 (GraphPad Software, San Diego, CA, USA). Results were considered statistically significant at $P < 0.05$.

E Mass spectrometry

The protein bands stained with silver were cut, de-stained, reduced with dithiothreitol, alkylated with IAA, and digested in-gel with trypsin. The resulting peptide mixtures were extracted in a buffer containing 50% acetonitrile and 5% trifluoroacetic acid, and analyzed by mass spectrometry using rat UniProtKB database and IDENTITY^{E}, which consists of nanoACQUITY, Xevo QTof MS and ProteinLynx^{TM} Global SERVER (PLGS) 2.5.2. (Nihon Waters K.K., Tokyo, Japan).

Ⅲ Results

The meshwork-like structures of PSD, such as PSD-lattice, have been reported since the 1970's in deoxycholate (DOC)-treated SPM[10)-13)]. Here, we observed the presence of mesh-like structures in the PSDs prepared under various conditions, such as treatment of SPM with high concentration of TX-100, in immature PSDs, and in PSDs obtained from snap frozen brains. Typical examples of electron micrographs (thin sections) of PSDs prepared under these different conditions are shown in **Fig. 2**. Arrows indicate typical lattice-like structures in PSD. PSDs prepared after treatment of SPM with 5%TX-100 appeared to unfold the tightly organized PSD structures (**Fig. 2B**). In immature PSDs (7-day-old), the basement backbones with meshwork-like structure, possibly before heavy association of varying PSD proteins, were visible (**Fig. 2C, D**). PSDs prepared from snap frozen brains displayed structures that were more scarce than the PSDs prepared from brains collected without immediate freezing, as we reported previously (**Fig. 2E, F**)[14]. These lattice-like structures were difficult to detect, in general, in the 1%TX-PSD and 1%OG-PSD prepared under regular conditions from adult brains, because of the densely packed proteins associated with mature PSDs (**Fig. 2A**).

In the negative staining of mature PSDs (6w-1%TX-PSD), no mesh-like structure was observed, which is probably due to the number of materials packed on them (**Fig. 3A**). In contrast to the 1%TX-PSD, it was easier to see the inside structure of PSD and meshwork-like structures in the case of 1%OG-PSDs (**Fig. 3B**). In the 5%TX-PSD from 6-week-old rats, some of the PSD structures tended

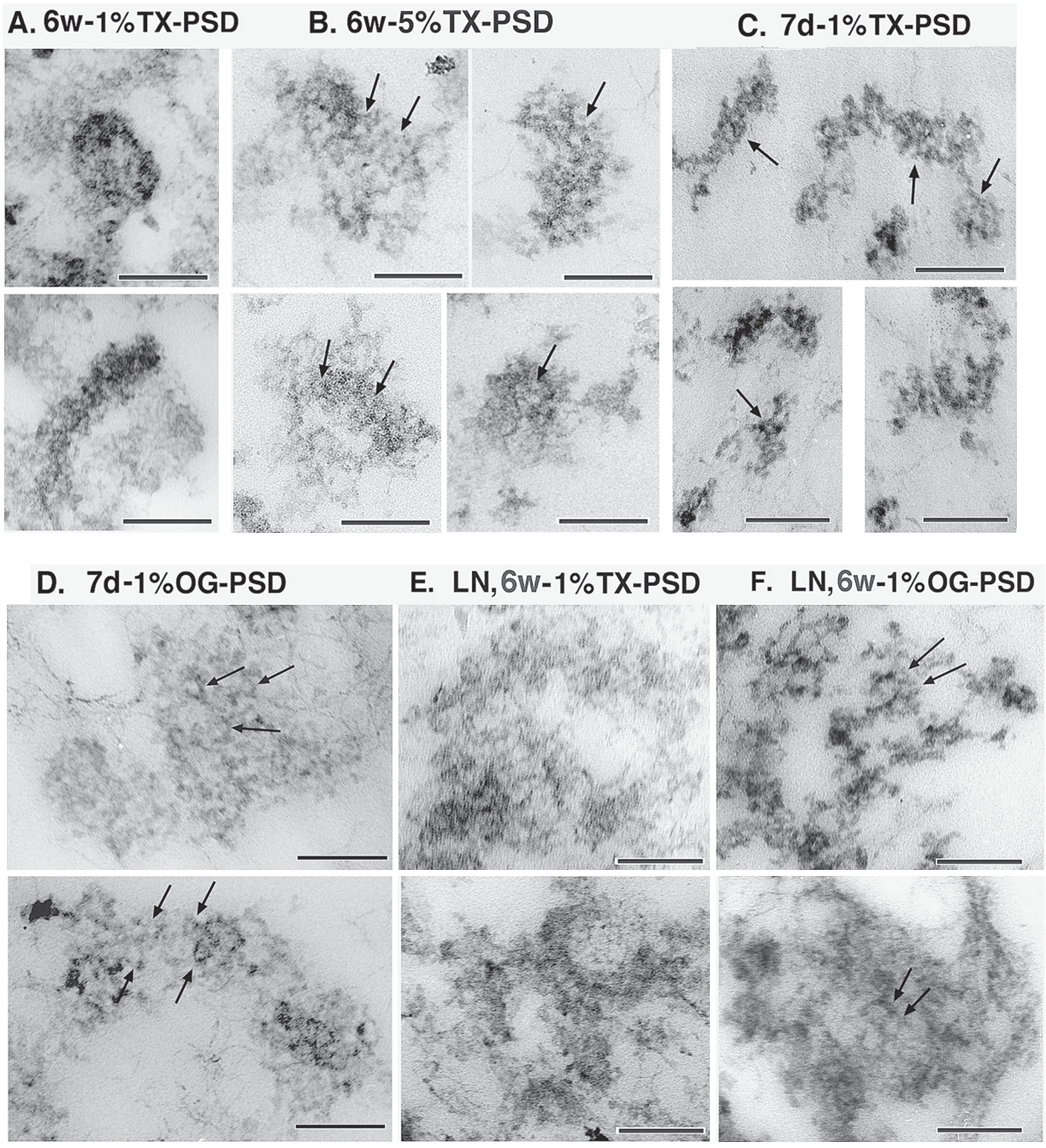

Fig. 2 Electron microscopic observation of various PSDs (thin section).

Typical examples of electron micrographs of PSDs purified under various conditions. Conditions are indicated at the top of the electron micrographs. Typical mesh-like structures are indicated with arrows. 6w (6-week-old) and 7d (7-day-old) indicate the ages of the rats. Scales are 200 nm. PSDs, postsynaptic densities.

to be unfolded and the lattice-like structures were disclosed (**Fig. 3C**). In 7d-1%TX-PSD (**Fig. 3D**), packing of fine molecules was observed, but not the lattice-like structures. In the 7d-1%OG-PSD (**Fig. 3E**) and 1%LN-PSD (both 1%TX- and 1%OG-PSDs) (**Fig. 3F, G**), structures inside the PSD were more clearly visible compared with 6w-1%TX-PSD, which suggested the formation of mesh-like or lattice-like structures.

Furthermore, we investigated the protein constituents of PSDs in which lattice-like structures were observed. Proteins in these PSDs were separated and visualized by silver staining (**Fig. 4 A, B**). According to the SDS-PAGE profile shown in **Fig. 4A**,

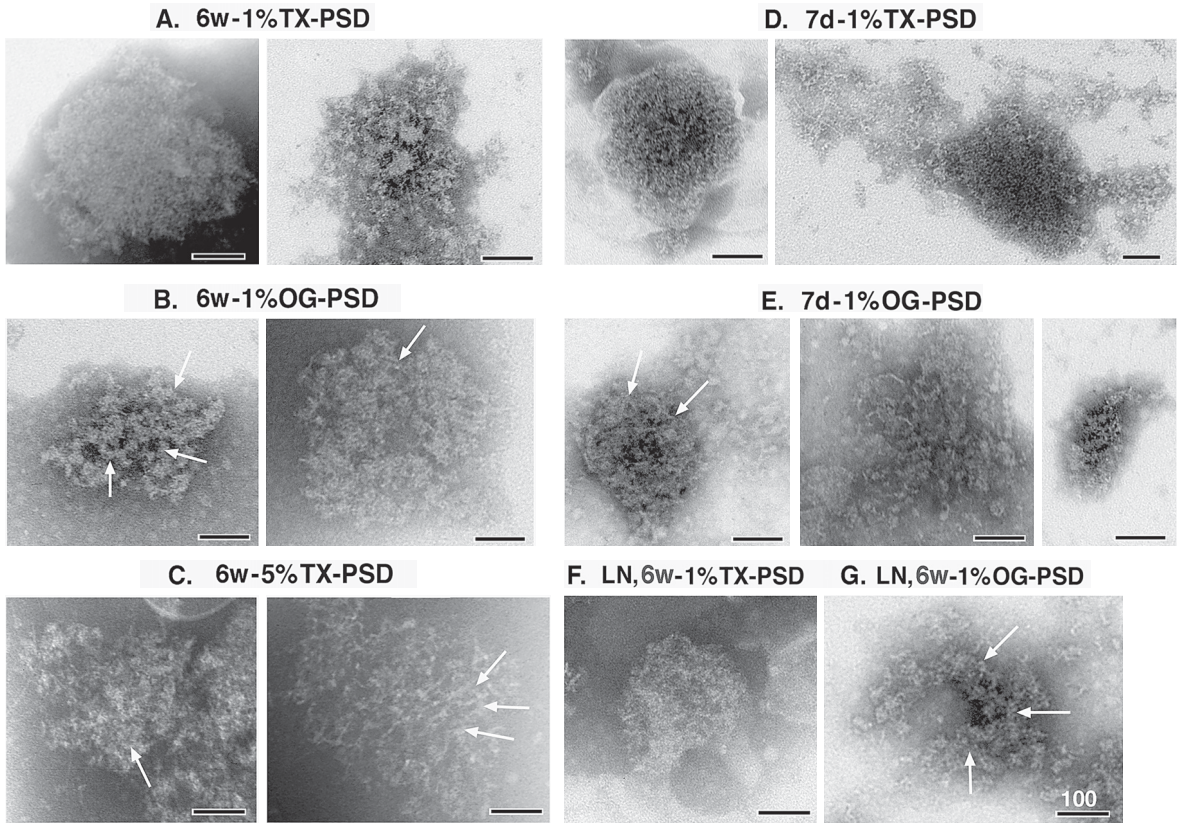

Fig. 3 Electron microscopic observation of various PSDs (negative staining).
Typical examples of electron micrographs of PSDs purified under various conditions. Conditions are indicated at the top of the micrographs. Arrows indicate typical mesh-like or lattice-like structures. PSDs in B, C, E, F and G appear to be entirely mesh-like. 6w (6-week-old) and 7d (7-day-old) indicate the ages of the rats. Scales are 100 nm. PSDs, postsynaptic densities.

concentrations of some proteins were high in 7d-PSD, in particular the 45-kDa protein in 7d-1%TX-PSDs and 45-kDa and 31-kDa proteins in 7d-1%OG-PSDs (open arrowheads in **Fig. 4A**). In LN-PSDs, protein recoveries were reduced compared with regularly prepared PSDs (lane marked "6w" in **Fig. 4B**). More specifically, CaMKIIα contents were reduced in both TX- and OG-PSDs prepared from snap frozen forebrains. In contrast, CaMKIIα was increased in TX- and OG-PSDs prepared from forebrains incubated at 37℃ for 5 min immediately after dissection (**Fig. 4B**). This result is in good agreement with our previous findings[14]. Moreover, the 31-kDa protein (arrow in **Fig. 4B**) was highly enriched in the OG-LN-PSD, as well as in other OG-PSDs.

Major proteins in these PSDs from 7-day-old and snap frozen forebrains were identified by mass spectrometry, and the results are indicated in the protein profiles visualized with enhanced silver staining (**Fig. 4C, D**; see also **Table 2**). The 45-kDa protein was identified as actin. The 31-kDa protein was a mixture of at least three proteins, ADP/ATP translocase (AAT), prohibitin, and 14-3-3, as reported previously[15], with AAT being the major one. Abundant cytoskeletal proteins, although less abundant than actin, included α-IN, neurofilament-L, and tubulin in the 7d-TX-PSD. Tubulins were also abundant in the 7d-OG-PSD, but to a lesser extent than actin. Moreover, α-IN was also detected in 7d-OG-PSDs, although to a lesser extent than in 7d-TX-PSDs. In the 1%TX-LN-PSD, bands including α-IN, actin, and tubulin were abundant. Similar to the 7d-OG-PSD, actin and 31-kDa protein were also abundant in the 1%OG-LN-PSD. Proteins other than the cytoskeletal proteins were also identified, but their involvement in the PSD structure remains to be clari-

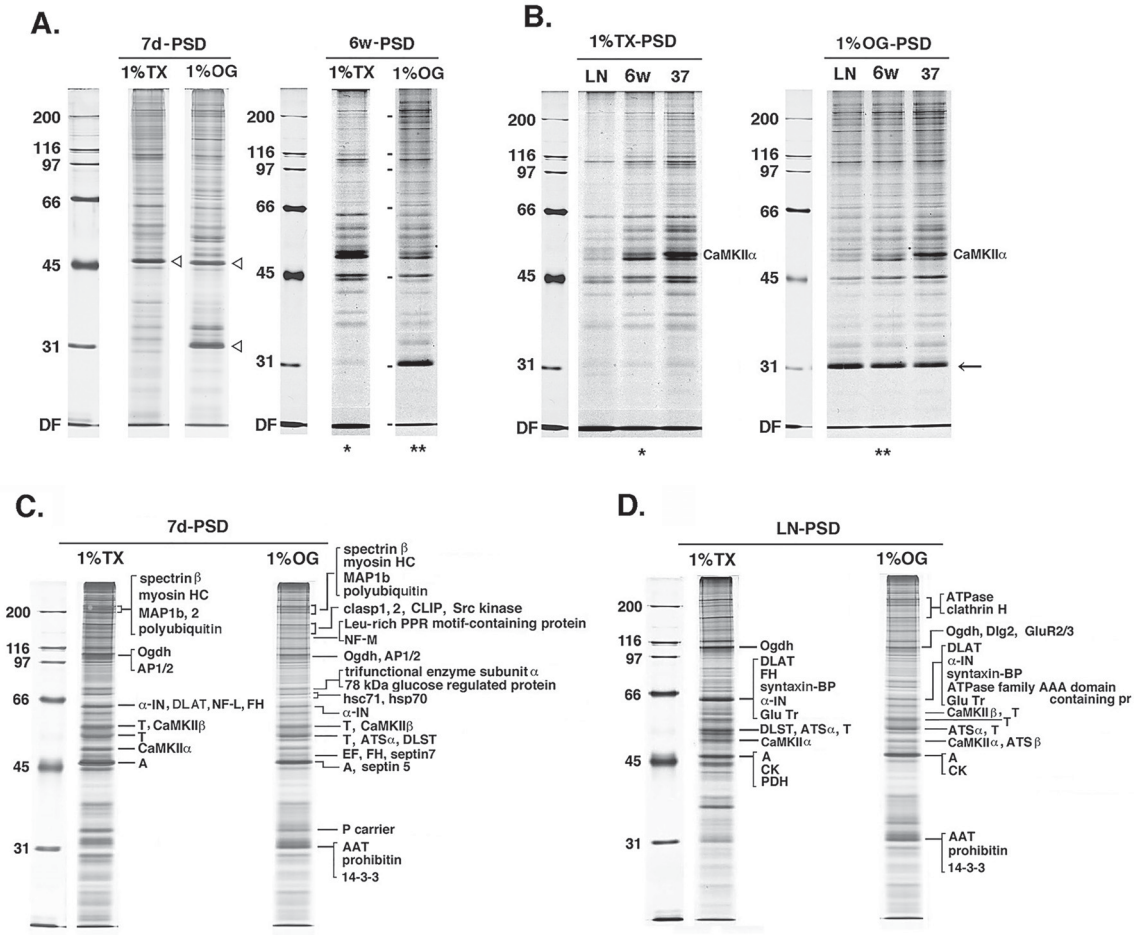

Fig. 4 Protein components of various PSDs.

A. Protein profiles of PSDs, in both 1%TX(Triton X)-100-PSD and 1%OG(n-Octyl-β-D-glucoside)-PSD, prepared from forebrains at 7-day-old and 6-week-old (7d and 6w, respectively). Protein amounts in each lane were adjusted by the corresponding total protein amount measured by densitometry of silver-stained lanes and analysis using NIH Image. Thus, protein amounts were the same in each lane. B. Protein profiles of PSDs, in both 1%TX-PSD and 1%OG-PSD, prepared from snap frozen forebrains with liquid nitrogen (LN), placed on ice for ～30 min or placed at 37 ℃ for 5 min after dissection (LN, 6w or 37, respectively). Equal volumes (20 μl) of PSD samples were loaded in each lane. C, D. Identification of major protein bands contained in the different PSDs using mass spectrometry. Silver staining was enhanced compared with those shown in A and B, and thus, the number of protein bands visible was increased. Numbers to the left of the gel images indicate molecular weights in kDa. Abbreviation of protein names : A, actin ; α-IN, α-internexin ; AAT, ADP/ATP translocase ; AP, Adaptor related protein complex ; ATS, ATP synthase ; CK, Creatine kinase ; clasp, CLIP-associating protein ; CLIP, cytoplasmic linker protein ; Dlg, Disks large homolog ; DLAT, Dihydrolipoyllysine residue acetyltransferase component of pyruvate dehydrogenase complex ; DLST, Dihydrolipoyllysine residue succinyltransferase component of 2 oxoglutarate dehydrogenase complex ; EF, elongation factor Tu or 1α ; FH, Fumarate hydratase ; Glu Tr, Glutamate transporter, hsc71, heat shock cognate 71 ; hsp70, heat shock protein 70 ; MAP, microtubule-associated protein ; myosin HC, myosin heavy chain ; NF-M, neurofilament-M ; Ogdh, oxoglutarate dehydrogenase ; P-carrier, phosphate carrier protein ; PDH, pyruvate dehydrogenase complex ; PSDs, postsynaptic densities ; syntaxin-BP, syntaxin-binding protein ; syntaxin-BP, syntaxin-binding protein ; T, tubulin. For details, see Table 1.

fied. Typical scaffold and adaptor proteins in the PSD were not identified by mass spectrometry of the major bands, possibly because of the small amounts.

The number of protein bands contained in the 5% TX-PSD was high (data not shown) as well as in 1% TX-PSD, although mesh-like PSD structures were observed in the former preparation. Although PSDs were highly unfolded, our observations suggest that many proteins were not extracted, but remained

Table 2

(1) List of the major proteins contained in the 7d-1%TX-PSD derived from forebrain SPM

Protein name	UniprotKB/Swiss-Prot
spectrin β	Q5D002
myosin HC (myosin heavy chain)	Q9JLT0
MAP1b	B0BNK3
MAP2	P15146, D3ZW41
polyubiquitin	Q63429, P0CG51
oxoglutarate dehydrogenase (Ogdh)	Q5XI78
Adaptor related protein complex (AP1/2)	P62944, Q3ZB97, P52303, P18484, Q66HM2, D3ZUY8
α-internexin (α-IN)	P23565
Dihydrolipoyllysine residue acetyltransferase component of pyruvate dehydrogenase complex (DLAT)	P08461
neurofilament H (NF-H)	P16884
Fumarate hydratase (FH)	Q5M964
Tubulin (T)	P68370, Q6P9V9, Q68FR8, Q6AYZ1, Q5XIF6, Q6AY56, Q4QRB4, P69897, P85108, Q3KRE8, Q6P9T8, Q4QQV0,
CaMKII β	P08413, Q63094
CaMKII α	P11275
Actin (A)	P63259, P60711, P63269, P68035, P62738, P68136

(2) List of the major proteins contained in the 7d-1%OG-PSD derived from forebrain SPM

Protein name	UniprotKB/Swiss-Prot
spectrin β	Q5D002
myosin HC (myosin heavy chain)	Q9JLT0
microtubule-associated protein 1b (MAP1b)	B0BNK3
polyubiquitin	Q63429, P0CG51
clasp1	Q5M928
clasp2	D3ZZU1, D4A289, D3ZG34
CLIP	Q99JD4
Src kinase	Q9QXY2
Leu-rich PPR motif-containing protein	Q5SGE0
neurofilament-M (NF-M)	P12839
oxoglutarate dehydrogenase (Ogdh)	Q5XI78
Adaptor related protein complex (AP1/2)	P62944, Q3ZB97, P52303
trifunctional subunit α	Q64428
78 kDa glucose regulated protein	P06761
heat shock cognate (hsc71)	P63018
heat shock protein (hsp70)	P55063
α-internexin (α-IN)	P23565
Tubulin (T)	P68370, Q6P9V9, Q6AYZ1, Q68FR8, Q5XIF6, Q6AY56, Q4QRB4, P85108, Q3KRE8, P69897, Q6P9T8, Q4QQV0
CaMKII β	P08413, Q63094
ATP synthase (ATS α)	P15999
Dihydrolipoyllysine residue succinyltransferase component of 2 oxoglutarate dehydrogenase complex (DLST)	D0VYQ0
EF	P85834, D3ZC88, P62630, D3ZRH9, D4A0X4, D3ZXS6, P62632
Fumarate hydratase (FH)	P14408, Q5M964
septin5	Q9JJM9
P-carrier	P16036
ADP/ATP translocase (AAT)	Q09073, Q05962
prohibitin	P67779
14-3-3 protein	P63102, P61983, P68511, P68255, P35213, P62260

(3) List of the major proteins contained in the LN,6w-1%TX-PSD derived from forebrain

SPM Protein name	UniprotKB/Swiss-Prot
oxoglutarate dehydrogenase (Ogdh)	D3ZQD3
Dihydrolipoyllysine residue acetyltransferase component of pyruvate dehydrogenase complex (DLAT)	P08461
Fumarate hydratase (FH)	P14408
syntaxin-binding protein (syntaxin-BP)	P61765
α-internexin (α-IN)	P23565
Glutamate transporter (Glu Tr)	Q8K5B5, Q91ZA9
Dihydrolipoyllysine residue succinyltransferase component of 2 oxoglutarate dehydrogenase complex (DLST)	Q01205, D0VYQ0
ATP synthase α (ATS α)	P15999
Tubulin (T)	P69897, Q4QRB4, Q3KRE8, P85108
α subunit of Ca2+/calmodulin-dependent protein kinase II (CaMKII α)	P11275
Actin (A)	P60711, P63259, P62738, P63269, P68136, P68035
creatin kinase (CK)	Q5BJT9, P25809
pyruvate dehydrogenase complex (PDH)	P26284, Q4FZZ4

(4) List of the major proteins contained in the LN,6w-1%OG-PSD derived from forebrain

SPM Protein name	UniprotKB/Swiss-Prot
ATPase	P06687, P06686, P06685, Q64541, Q5PQV3,
clathrin H	P11442
oxoglutarate dehydrogenase (Ogdh)	Q5XI78
Disks large homolog2 (Dlg2)	Q63622, D4AA89
Glutamate receptor 2/3 (GLuR2/3)	P19491, P19492
Dihydrolipoyllysine residue acetyltransferase component of pyruvate dehydrogenase complex (DLAT)	P08461
α-internexin (α-IN)	P23565
syntaxin-binding protein (syntaxin-BP)	P61765
ATPase family AAA domain containing protein	Q3KRE0
Glutamate transporter (Glu Tr)	Q8K5B5, Q91ZA9
CaMKII β	P08413, Q63094
Tubulin (T)	Q6P9V9, P68370, Q6AYZ1, Q5XIF6, Q68FR8, Q6AY56, Q4QRB4, P85108, Q3KRE8, P69897, Q6P9T8, Q4QQV0
ATP synthase α (ATS α)	P15999
CaMKII α	P11275
ATP synthase β (ATS β)	P10719
Actin (A)	P60711, P63259, P62738, P68035, P68136, P63269
creatin kinase (CK)	Q5BJT9
ADP/ATP translocase (AAT)	Q09073, Q05962
prohibitin	P67779
14-3-3 protein	P63102, P61983, P68511, P68255, P62260

attached to the PSD core structures after treatment with high concentrations of TX-100.

Subsequently, we carried out western blotting to compare the concentrations of typical PSD proteins in various PSD preparations. In particular, we compared between 7d-PSD and 6w-PSD and between LN- and 6w-PSD, focusing on scaffold/adaptor proteins and cytoskeletal proteins. Figures 5 and 6 illustrate representative western blots and their quantitated results. In the comparison between 7d- and 6w-PSDs (**Fig. 5**), concentrations of scaffold and adaptor proteins, except for SAP102, were very low in both 7d-TX-PSDs and 7d-OG-PSD. The concentration of SAP102 was comparable between 7d- and 6w-PSDs. The concentration of Shank1 was also comparable between 7d-TX- and 6w-TX-PSDs, while it decreased in 7d-OG-PSDs. These results are in good agreement with the developmental changes in the expression of these proteins in the brain and synapses. In particular, early developmental expression of SAP102[16)-18)] and some type of Shank[16)18)] supports our results. The concentration of cytoskeletal proteins in 7d-PSDs was equal to or higher than in 6w-PSDs, except for NF-H (**Fig. 5B**). Moreover, concentrations of actin and α-IN were significantly high in OG-PSDs prepared from 7d-old forebrains, although not significant in TX-PSDs. Concentrations of CaMKII α and CaMKII β in 7d-PSDs were lower than those in 6w-PSDs (**Fig. 5C**). This result is in agreement with the developmental changes of CaMKII expression in the brain and synapses[19)].

Fig. 6 illustrates the concentrations of scaffold and adaptor proteins in 6w-LN- and 6w-PSDs. Concentrations of chapsyn-110 appeared to be high in both TX- and OG-LN-PSDs. The concentration of SAP102 was significantly higher in LN-TX-PSDs compared with 6w-TX-PSDs, whereas there was no difference between LN-OG- and 6w-OG-PSDs. The difference between the OG- and TX-PSDs could be caused by the different properties of the two detergents. Other scaffold and adaptor proteins appeared to be the same between LN- and 6w-PSDs. Concentrations of the cytoskeletal proteins examined were not significantly different between LN- and 6w-PSDs. Thus, most of the scaffold/adaptor proteins and cytoskeletal proteins examined in LN-PSDs were at the same level with 6w-PSDs. Chapsyn-110 and SAP102 were concentrated exceptionally in LN-PSDs for unknown reasons. Concentrations of CaMKII α and CaMKII β in LN-PSDs were lower than in 6w-PSDs in both TX- and OG-PSDs. The results of the quantitative study are summarized in **Table 3**.

Ⅳ Discussion

The presence of meshwork-like structures was demonstrated under various conditions, such as extreme solubilization of PSDs (e.g., with 5% TX-100 or DOC) and PSDs prepared from snap frozen brains using LN. Snap freezing and 37 ℃-treatment of the dissected brains result in thinning and thickening of PSD, respectively. Thinning or thickening of PSD is mainly due to scantiness or abundance of CaMKII[14)]. Following brain dissection, CaMKII is activated by Ca^{2+} influx into damaged neurons, which causes autophosphorylation and clustering of the kinase, and finally accumulation into PSD[20)]. This postmortem effect is enhanced by incubation of dissected brains at 37 ℃ causing augmented thickening of PSD. In this paper, we used snap freezing to prepare thin PSD in order to search for its essential components.

Electron microscopic analyses of 7d-PSDs suggested that meshwork-like structures are already formed in the early synaptogenesis stage[10)-13)]. Similar intercalating PSD fiber network structures have been clearly shown in a synaptic complex prepared using p-iodonitrotetrazolium and further treated with urea (1 or 8 M) and mild sonication[21)]. It is likely that p-iodonitrotetrazolium used in order to exclude mitochondrial contamination unintentionally cross-linked the PSD structure through oxidation. Thus, it prevented the disorganization of the PSD basic core structure when treated with high concentrations of urea, which dissociates most of the proteins that are attached to the PSD core. PSD proteins other than those constructing PSD core structures may be very densely attached to the core structure. This makes the mesh-like structures underneath rarely detectable in regularly prepared PSDs in both

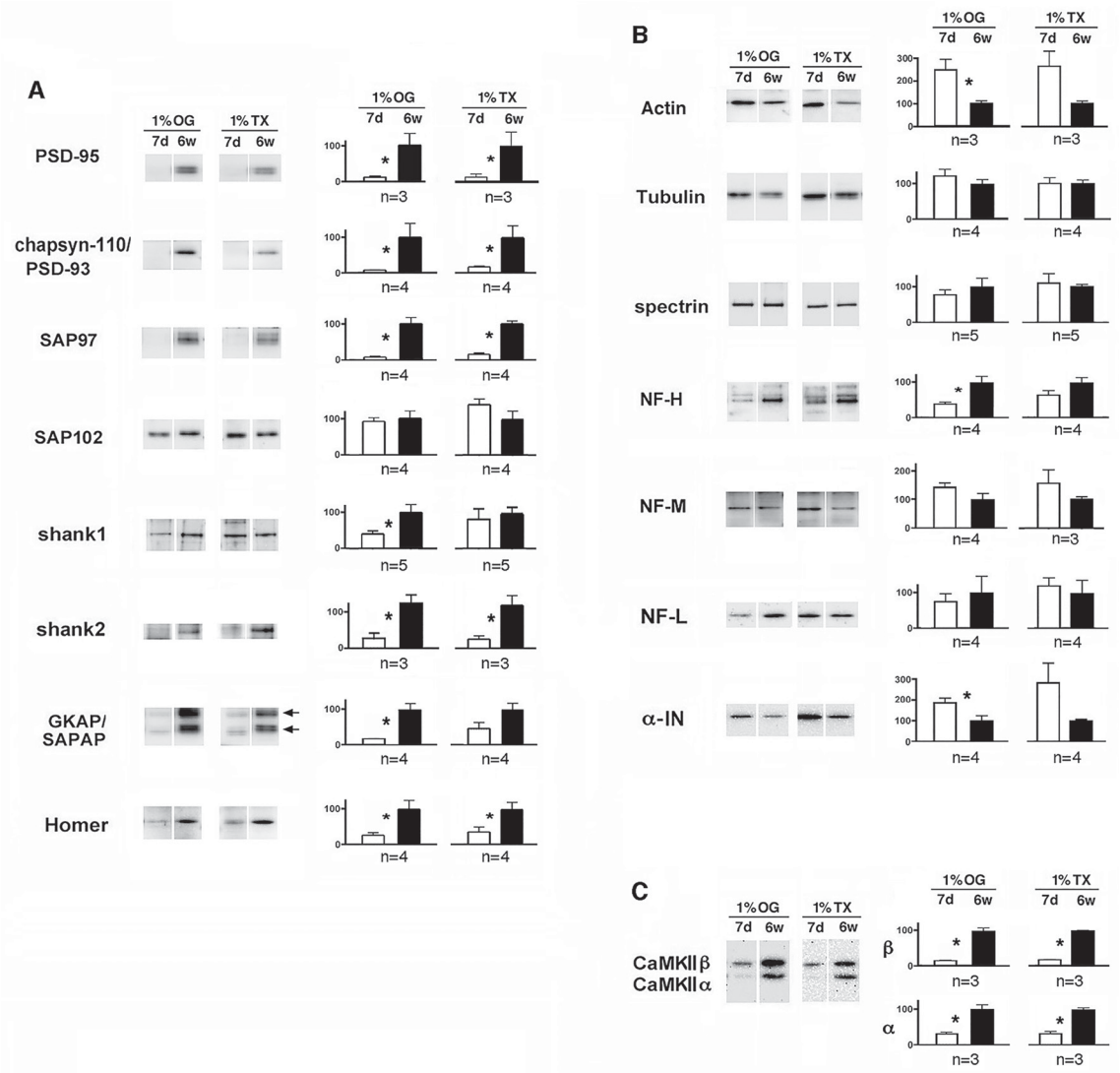

Fig. 5 Western blot analysis of typical PSD proteins contained in the PSDs prepared from 7-day-old rat forebrains (7d) compared with those in 6w-PSDs (6w).

A. Scaffold and adaptor proteins. B. Cytoskeletal proteins. C. Ca^{2+}/calmodulin-dependent protein kinase II (CaMKII). Same amounts of proteins in the 7d-, LN- and 6w-PSD were run on a single gel. Western blotting of 7d-, LN- and 6w-PSD was carried out in the same blot, and conditions visualizing the immunoreactive bands are the same in each comparison. Immunoreactivity was measured by densitometry using video CCD camera and quantified by ATTO lane analyzer, and ratios against the values of standard band were sought. The averaged values of the ratios of 6w-1%OG (n-Octyl-β-D-glucoside) and 6w-1%TX (Triton X), respectively, were set at 100%. Vertical values (means ± standard error of mean) represent percentage of the signals to those of 6w-1%OG and 6w-1%TX. *P<0.05, unpaired Student's test (two-tailed). Arrows indicate 95-kDa GKAP protein and 110-kDa immunoreactive protein, as commented on by the manufacturer. Only 95-kDa bands were quantitated. Abbreviations of the protein names are the same as those in Fig. 4 legend. PSD, postsynaptic density.

regular thin sections and negatively stained electron micrographs (partly shown in **Fig. 2, 3**). In the 7d-PSDs, relatively few proteins were associated with the core mesh-like structure, which enabled its visualization. Mesh-like structures similar to PSD lattice were also indicated in the platinum-shadowed adult PSDs[22], and in purified immature and mature PSDs by electron cryotomography[23]. Therefore, the meshwork structure does not appear to be an artifact produced after treatment of synapses with detergents. Thus, this experiment supports the idea that the mesh-like structure is present underneath

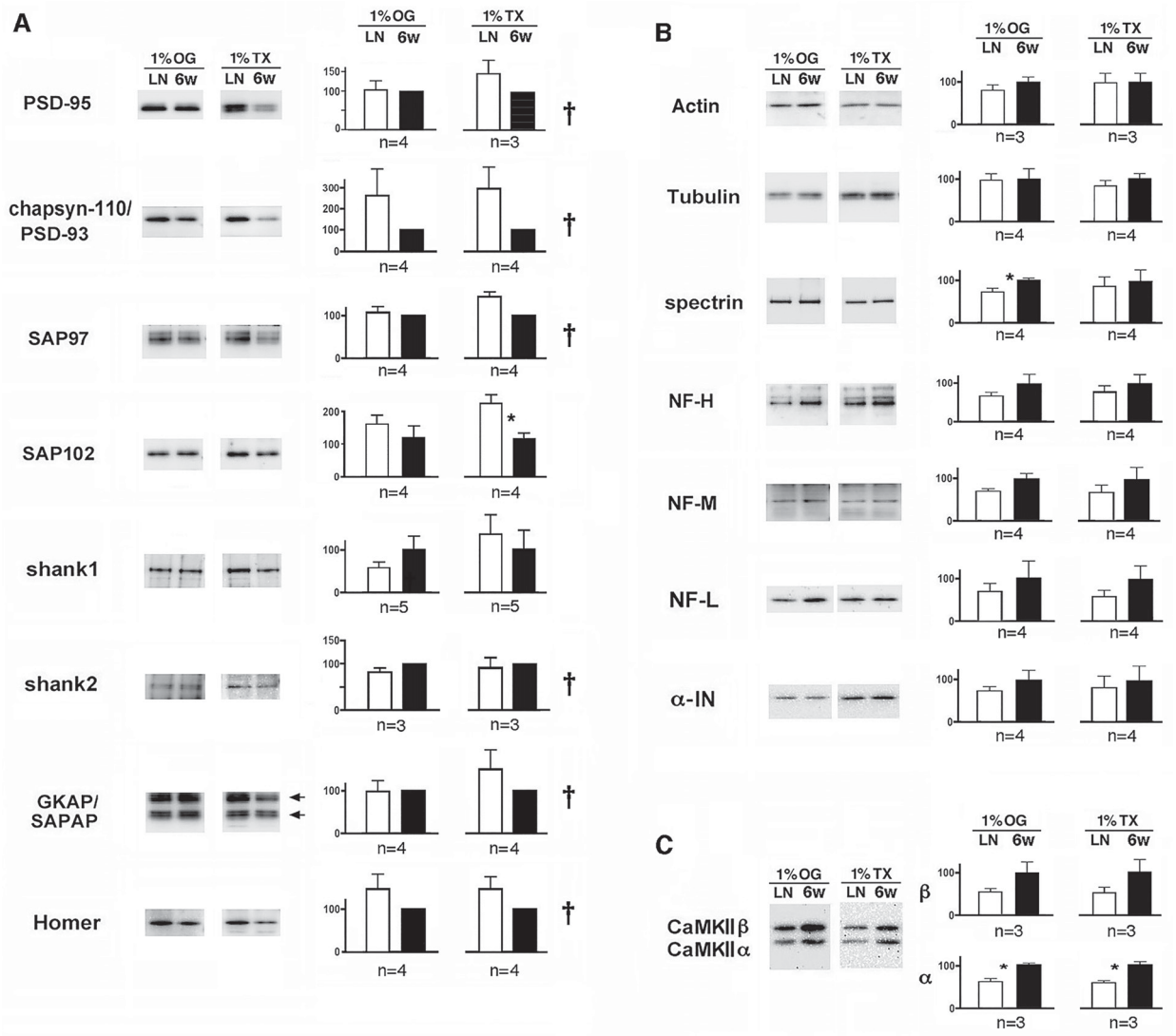

Fig. 6 Western blot analysis of typical PSD proteins contained in the PSDs prepared from LN-treated forebrains (LN) compared with those in 6w-PSDs.

A. Scaffold and adaptor proteins. B. Cytoskeletal proteins. C. Ca^{2+}/calmodulin-dependent protein kinase II (CaMKII). Experiment was carried out as described in Fig. 5 legend. Vertical values (means ± standard error of mean) represent percentage of the signals to those of 6w-1%OG (n-Octyl-β-D-glucoside) and 6w-1%TX (Triton X). In the cases indicated by †, where standard values were extremely low, ratios of LN-PSD vs. 6w-PSD values were processed to avoid high extent of variation of the final ratios. Thus, values in the 6w-PSD columns are fixed to 100% with no error bars. *P<0.05, unpaired Student's test (two-tailed). PSD, postsynaptic density.

the PSD and that it is a core PSD structure. The meshwork-like structure mentioned above may be the same as the PSD lattice, which was first reported in the 1970's.

It is believed that different types of scaffold and adaptor proteins are interwoven to make PSD lattice-like network structures. However, there has been no sound evidence supporting this concept. We also do not know whether the PSD lattice is composed mainly of scaffold and adaptor proteins or whether other proteins also play a major role. Major or key components and the molecular organization of the PSD lattice have not yet been identified because there remain a number of proteins in the DOC-insoluble PSD lattice preparations[10)13)]. Therefore, in this work, we surveyed the key components that construct the core structure of PSD. Firstly, we compared the protein profiles between regularly

	7d-PSD	LN, 6w-PSD
SAP102	～	↑
chapsyn-110	↓	↑
other sc/ad proteins	↓	～
actin & α-IN	↑	～
other CSK proteins	～	～
CaMKII	↓	↓

Table 3 Changes in protein amounts in 7d- and LN-PSDs compared with regular mature PSDs (6w-PSDs)
sc/ad proteins, scaffold and adaptor proteins; CSK proteins, cytoskeletal proteins; (～), same level

prepared PSDs and those enriched with mesh-like structures ("regular preparation").

In 7d-1%TX-PSD, actin was the most abundant protein, while 7d-1%OG-PSDs were enriched with both actin and 31-kDa proteins. AAT, the major component of the 31-kDa proteins, did not appear to be localized to PSD, because pre-embedding electron microscopic examination did not detect any signals of ATT in the PSD (data not shown). In both TX- and OG-LN-PSDs, CaMKII content was extremely diminished as reported previously[14], but no apparent changes were observed in other proteins as far as silver-stained protein profiles were concerned. Unfortunately, a number of proteins were still observed in these 7d- and LN-PSDs as well as in the regularly prepared adult PSDs in a one-dimensional gel electrophoresis when the silver staining was enhanced (**Fig. 4C, D**). Therefore, it was difficult to identify key components or acquire information on the molecular organization of the PSD core structure even after mass spectrometry of protein bands of both 7d- and LN-PSDs.

Subsequently, we focused on the PSD scaffold-adaptor proteins and cytoskeletal proteins, and compared their contents between regularly prepared adult PSDs and those enriched with mesh-like structures by western blot-based quantitation. The results are summarized in **Table 3**. In the 7d-PSDs, contents of scaffold and adaptor proteins, except for SAP102, were extremely low. This was also the case for CaMKII α and CaMKII β. These differences may reflect developental changes in the expression of these proteins. It is well known that there is a developmental switch in the expression level from SAP102 to PSD-95, which means that SAP102 expression is present primarily in the younger age among all the PSD-95-like subfamily of the membrane-associated guanylate kinase (MAGuk) proteins (PSD-95, PSD-93, SAP102, and SAP97)[24]. Thus, it is possible that, instead of PSD-95, it is SAP102 that plays a role in the PSD core formation and maintenance in immature PSDs. The concentration of Shank1 in 7d-TX-PSD was at the same level as the 6w-TX-PSD, although the reason remains unknown. In contrast, the concentrations of general cytoskeletal proteins, except for NF-H in OG-PSD, were the same or even higher in the immature PSD fractions compared with regularly prepared adult PSDs. These results suggest an involvement of general cytoskeletal proteins, except for NF-H, in the core structure of immature PSDs. In particular, actin and α-IN may play major roles in the formation of PSD lattice/meshwork. As for NF-H, it has been reported, together with NF-M, not to be a constituent of PSD[25].

In the comparison between LN- and 6w-PSDs, both most scaffold-adaptor proteins and general cytoskeletal proteins were comparable with the adult PSD. Chapsyn-110 and SAP102 were concentrated in LN-PSDs. The levels of CaMKII, in particular the α isoform, were decreased compared with regularly prepared PSDs, which is in line with our previous findings[14]. These results suggest that both scaffold-adaptor proteins and general cytoskeletal proteins are part of the core structure proteins in mature PSDs. It appears that brain snap freezing prevents tight association of CaMKII with PSDs and reduces relatively specifically CaMKII in particular, and possibly CaMKII protein complexes as well, in LN-PSD preparations. CaMKII forms clusters and make PSDs highly electron-dense if associated with

PSDs, as shown in thickened PSDs[14]. In LN-PSDs, internal structures could be visualized by the absence of most CaMKII and CaMKII clusters.

In summary, our results suggest a role of general cytoskeletal proteins, in particular actin and α-IN, and SAP102 in the formation of immature and nascent PSDs by constructing the PSD core structure. In contrast, scaffold proteins, such as PSD-95, chapsyn110/PSD-93, SAP97, Shank, GKAP, and Homer seem to play major roles in mature PSDs, but not in immature PSDs. Moreover, CaMKII may also not play a major role in the PSD mesh-like core structure. Further analyses using different approaches are expected.

Acknowledgements

We acknowledge Dr. K. Kametani, Shinshu University, for help with electron microscopy and Dr. Fujii, Shinshu University, for the generous gift of anti-tubulin antibody. This work was funded by two grants (to T.S.) from the Institute for Biomedical Sciences, Interdisciplinary Cluster for Cutting Edge Research, Shinshu University, and the Institute of Medicine, School of Medicine and Health Sciences, Shinshu University Academic Assembly, in addition to a grant (to W.G.) from Shinshu Public Utility Foundation for Promotion of Medical Sciences. We would like to thank Editage (www.editage.jp) for English language editing.

Declarations of Interest

The authors have no conflicts of interest to declare.

References

1) van Bokhoven H : Genetic and epigenetic networks in intellectual disabilities. Annu Rev Genet 45 : 81-104, 2011
2) Suzuki T, Tian QB, Kuromitsu J, Kawai T, Endo S : Characterization of mRNA species that are associated with postsynaptic density fraction by gene chip microarray analysis. Neurosci Res 57 : 61-85, 2007
3) Ting JT, Peca J, Feng G : Functional consequences of mutations in postsynaptic scaffolding proteins and relevance to psychiatric disorders. Annu Rev Neurosci 35 : 49-71, 2012
4) Bosch M, Castro J, Saneyoshi T, Matsuno H, Sur M, Hayashi Y : Structural and molecular remodeling of dendritic spine substructures during long-term potentiation. Neuron 82 : 444-459, 2014
5) Baron MK, Boeckers TM, Vaida B, Faham S, Gingery M, Sawaya MR, Salyer D, Gundelfinger ED, Bowie JU : An architectural framework that may lie at the core of the postsynaptic density. Science 311 : 531-535, 2006
6) Suzuki T : Isolation of synapse-subdomains by subcellular fractionation using sucrose density gradient centrifugation. Neuroproteomics "Springer Protocols Neuromethods, (Li KW, eds), Humana Press (New York) 57 : 47-61, 2011
7) Zhao L, Sakagami H, Suzuki T : Detergent-dependent separation of postsynaptic density, membrane rafts and other subsynaptic structures from the synaptic plasma membrane of rat forebrain. J Neurochem 131 : 147-162, 2014
8) Du F, Saitoh F, Tian QB, Miyazawa S, Endo S, Suzuki T : Mechanisms for association of Ca^{2+}/calmodulin-dependent protein kinase II with lipid rafts. Biochem Biophys Res Commun 347 : 814-820, 2006
9) Suzuki T, Zhang J, Miyazawa S, Liu Q, Farzan MR, Yao WD : Association of membrane rafts and postsynaptic density : proteomics, biochemical, and ultrastructural analyses. J Neurochem 119 : 64-77, 2011
10) Matus AI, Taff-Jones DH : Morphology and molecular composition of isolated postsynaptic junctional structures. Proc R Soc Lond B Biol Sci 203 : 135-151, 1978
11) Matus AI, Walters BB : Ultrastructure of the synaptic junctional lattice isolated from mammalian brain. J Neurocytol 4 : 369-375, 1975
12) Matus A : The postsynaptic density. Trends Neurosci 4 : 51-53, 1981
13) Blomberg F, Cohen RS, Siekevitz P : The structure of postsynaptic densities isolated from dog cerebral cortex. II.

Characterization and arrangement of some of the major proteins within the structure. J Cell Biol 74 : 204–225, 1977

14) Suzuki T, Okumura-Noji K, Tanaka R, Tada T : Rapid translocation of cytosolic Ca^{2+}/calmodulin-dependent protein kinase II into postsynaptic density after decapitation. J Neurochem 63 : 1529–1537, 1994

15) Liu Q, Yao W-D, Suzuki T : Specific interaction of postsynaptic densities with membrane rafts isolated from synaptic plasma membranes. J Neurogenet 27 : 43–58, 2013

16) Zheng CY, Seabold GK, Horak M, Petralia RS : MAGUKs, synaptic development, and synaptic plasticity. Neuroscientist 17 : 493–512, 2011

17) Sans N, Petralia RS, Wang YX, Blahos J 2nd, Hell JW, Wenthold RJ : A developmental change in NMDA receptor-associated proteins at hippocampal synapses. J Neurosci 20 : 1260–1271, 2000

18) Petralia RS, Sans N, Wang YX, Wenthold RJ : Ontogeny of postsynaptic density proteins at glutamatergic synapses. Mol Cell Neurosci 29 : 436–452, 2005

19) Kelly PT, Shields S, Conway K, Yip R, Burgin K : Developmental changes in calmodulin-kinase II activity at brain synaptic junctions : alterations in holoenzyme composition. J Neurochem 49 : 1927–1940, 1987

20) Hudmon A, Lebel E, Roy H, Sik A, Schulman H, Waxham MN, De Koninck P : A mechanism for Ca^{2+}/calmodulin-dependent protein kinase II clustering at synaptic and nonsynaptic sites based on self-association. J Neurosci 25 : 6971–6983, 2005

21) Cotman CW, Taylor D : Isolation and structural studies on synaptic complexes from rat brain. J Cell Biol 55 : 696–711, 1972

22) Petersen JD, Chen X, Vinade L, Dosemeci A, Lisman JE, Reese TS : Distribution of postsynaptic density (PSD)-95 and Ca^{2+}/calmodulin-dependent protein kinase II at the PSD. J Neurosci 23 : 11270–11278, 2003

23) Swulius MT, Farley MM, Bryant MA, Waxham MN : Electron cryotomography of postsynaptic densities during development reveals a mechanism of assembly. Neuroscience 212 : 19–29, 2012

24) Elias GM, Elias LA, Apostolides PF, Kriegstein AR, Nicoll RA : Differential trafficking of AMPA and NMDA receptors by SAP102 and PSD-95 underlies synapse development. Proc Natl Acad Sci U S A 105 : 20953–20958, 2008

25) Suzuki T, Mitake S, Okumura-Noji K, Shimizu H, Tada T, Fujii T : Excitable membranes and synaptic transmission : postsynaptic mechanisms. Localization of alpha-internexin in the postsynaptic density of the rat brain. Brain Res 765 : 74–80, 1997

(2017. 3. 3 received ; 2017. 4. 10 accepted)